مجلة جامعة الزاوية للعلوم الطبيعية
University of Zawia Journal of Natural Sciences *(UZJNS)*
https://journals.zu.edu.ly/index.php/UZJNS ISSN: 3078-4999

Effect of low- temperature annealing on the optical and electrical properties of near-infrared photosensors based on colloidal quantum dots

Wafaa F Gebril[a]

[a]*Department of Physics, Faculty of Sciences, University of Benghazi, Almarj, Libya*

**Corresponding email address:* gebrilwafaa@gmail.com

Received 06 May 2026 | Accepted 20 Sep 2026 | Available online 21 Sep 2026 | DOI: 10.26629/uzjns.2026.07

A B S T R A C T

The effect of low-temperature annealing on the electrical and optical properties of near-infrared photosensors based on colloidal PbSe nanocrystals capped with mercaptoacetic acid was investigated. The PbSe nanocrystals were synthesized via the hot-injection method, and their optical bandgap was determined to be approximately 0.78 eV from the optical absorbance spectrum. The electrical performance of the fabricated photosensors was evaluated by measuring their current–voltage (I–V) characteristics before and after annealing under nitrogen and air atmospheres. Additionally, the optical response of the devices was examined by measuring their spectral responsivity before and after air annealing. The PbSe nanocrystal device perfectly detected the near-infrared spectrum, and its performance was significantly improved after low-temperature air annealing. 60 °C air annealing enhanced the detectivity of the device by approximately 35% compared to its room-temperature detectivity.

Keywords: *colloidal PbSe nanocrystals, low-temperature annealing, near-infrared photosensors, PbSe nanocrystals.*

تأثير التلدين عند درجات حرارة منخفضة على الخصائص البصرية والكهربائية لأجهزة الاستشعار الضوئية لمنطقة الأشعة تحت الحمراء القريبة المبنية على النقاط الكمومية الغروانية

وفاء جبريل

قسم الفيزياء، كلية العلوم، جامعة بنغازي، المرج، ليبيا

الملخص

تمت دراسة تأثير التلدين عند درجات حرارة منخفضة على الخصائص الكهربائية والبصرية لأجهزة حساسات ضوئية تعمل بالأشعة تحت الحمراء القريبة، والمبنية على نقاط كمومية من سيلينيد الرصاص الغرواني المغطى بحمض المركابتواسيتيك. تم تصنيع بلورات سيلينيد الرصاص النانوية باستخدام طريقة الحقن الساخن، وتم تحديد فجوة الطاقة لها بحوالي 0.78 إلكترون فولت من طيف الامتصاص الضوئي. تم تقييم الأداء الكهربائي لأجهزة الاستشعار الضوئية المصنعة بقياس خصائص التيار-الجهد (**I-V**) قبل وبعد التلدين في جو من النيتروجين والهواء. بالإضافة إلى ذلك، تم فحص الاستجابة البصرية للأجهزة بقياس استجابتها الطيفية قبل وبعد التلدين في الهواء. استشعر جهاز بلورات سيلينيد الرصاص النانوية طيف الأشعة تحت الحمراء القريبة بكفاءة عالية، وتحسن أداؤه بشكل ملحوظ بعد التلدين في الهواء عند درجة حرارة منخفضة. أدى التلدين في الهواء عند 60 درجة مئوية إلى زيادة حساسية الجهاز بنسبة 35% تقريبًا من حساسيته عند درجة حرارة الغرفة.

الكلمات المفتاحية: *بلورات نانوية من سيلينيد الرصاص، مستشعرات ضوئية، تلدين بدرجة حرارة منخفضة، الأشعة تحت الحمراء القريبة، نقاط كمومية غروانية.*

1. Introduction

Near-infrared (NIR) photosensors play a crucial role in a variety of technologies, including biomedical diagnostics, optical communication systems, night-time imaging, and light energy harvesting applications [1]-[4]. The continued expansion and increasing breadth of these fields have created growing pressure to improve device performance, particularly by addressing limitations associated with current material platforms and device architectures [5], [6]. In this context, emerging semiconductor nanomaterials have attracted considerable attention for optoelectronic applications, including photosensing, due to their enhanced optical and electronic characteristics [7]-[9]. Among these, colloidal nanocrystals such as PbSe, PbS, and HgTe offer significant advantages, as they can be synthesized through solution-based methods with relatively simple processing requirements. These nanocrystals can be dispersed in solvents to form inks, enabling large-area film deposition using low-cost, low-temperature techniques such as spin coating. Furthermore, their compatibility with a wide range of

substrates—including silicon, glass, and flexible platforms—makes them particularly attractive for scalable and versatile device integration [10]-[12]. Over the past decades, a variety of photosensor devices based on colloidal nanocrystals have been developed, including photodiodes, photoconductors, and phototransistors [6]. The performance of these devices strongly depends on charge transport within the semiconductor films, which plays a critical role in their operation. Colloidal nanocrystals, also referred to as quantum dots (QDs), such as PbSe and PbS, have been widely investigated due to their distinctive optical behavior. One of their key advantages is the ability to tailor their bandgap by adjusting particle size, enabling sensitivity across a broad range of infrared wavelengths [6], [13]-[15]. Despite these benefits, the synthesis process typically involves surface ligands composed of long-chain organic molecules, which act as insulating barriers between adjacent nanocrystals and hinder charge transport. To address this limitation, various post-synthesis treatments have been explored to facilitate carrier movement within nanocrystal films [16], [17]. Among these approaches, thermal annealing has been identified as a straightforward and effective strategy for improving film conductivity [18]. In a related study, [19] demonstrated that annealing PbSe quantum dots capped with an oleic acid shell can significantly enhance transistor performance. Their results showed that the measured current increased from nearly negligible levels to a few picoamperes after treatment. In parallel, ligand exchange has emerged as an effective strategy for improving film conductivity by replacing long insulating ligands with shorter alternatives. Various substituting ligands have been explored for this purpose, including thiols, amines, and a range of inorganic species [16].

In this work, we present an improvement in the electrical and optical performance of near-infrared photosensors based on PbSe nanocrystals functionalized with mercaptoacetic acid (MAA) through a low-temperature annealing process. The PbSe colloidal nanocrystals were synthesized using a hot-injection technique, followed by a ligand exchange step to substitute the original oleic acid (OA) ligands with MAA.

The optical properties of the nanocrystals were evaluated using absorbance measurements, from which the bandgap was determined. Photosensor devices were then fabricated employing interdigital electrode structures. Their electrical behavior was characterized through current–voltage (I–V) measurements, while the photoresponse was analyzed by examining the spectral responsivity.

2. Experimental methods

Lead selenide (PbSe) quantum dots were synthesized following a previously reported hot-injection procedure [20], with slight modifications to the reaction conditions to achieve the desired properties. In the first step, a selenium precursor was prepared by dissolving selenium powder (8 mmol) in a mixture of n-trioctylphosphine (8 mL) and diphenylphosphine (60 µL). The solution was stirred under nitrogen at 60 °C overnight to ensure complete dissolution. Separately, the lead precursor was obtained by combining lead oxide (2 mmol), oleic acid (2.1 mL), and 1-octadecene (10.6 mL) in a three-neck flask, followed by heating at 140 °C for 1 hour under nitrogen flow. Once the solution became clear and colorless, indicating precursor formation, the selenium solution was rapidly injected to initiate quantum dot growth. After a reaction time of 40 s, the mixture was quickly cooled to room temperature using a water bath to quench further growth. The resulting quantum dots were purified by adding acetone, followed by centrifugation at 6000 rpm for 6 minutes, repeated three times to remove unreacted species and excess ligands. Subsequently, a ligand exchange process was performed to replace long-chain oleic acid ligands with shorter mercaptoacetic acid (MAA) molecules to enhance charge transport within the quantum dot film. For this purpose, the as-synthesized PbSe quantum dots were dispersed in excess MAA and stirred continuously at 70 °C for 48 hours under an inert atmosphere inside a glovebox. After ligand exchange, the quantum dots were further purified twice with acetone and dried under vacuum. Finally, the optical properties of the synthesized quantum dots were characterized by recording their absorbance spectra at room temperature using a Cary 500 UV–Vis–NIR spectrophotometer.

Photosensor devices were fabricated using gold interdigital electrodes deposited on a glass substrate. A schematic of the device structure is illustrated in Figure 1, where *w* denotes the width of each interdigital metal finger, while *d* represents the spacing between adjacent fingers. Standard optical photolithography was employed to define the electrode pattern on the substrate.

A 20 nm titanium (Ti) adhesion layer was first deposited using an electron-beam evaporator, followed by a 30 nm gold (Au) layer. Subsequently, PbSe quantum dots dispersed in chloroform were drop-cast onto the patterned electrodes to form the active sensing layer.

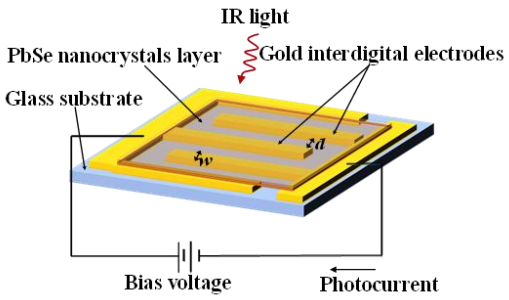

Figure 1. Schematic diagram of the fabricated photosensor structure.

The electrical response of the devices was evaluated by recording I–V characteristics using a Keithley 4200 semiconductor parameter analyzer. In addition, the optical response was investigated by recording the spectral responsivity using a Bruker IFS 125HR Fourier-transform spectrometer.

3. Results and Discussion

The absorbance spectra for the as-synthesized PbSe quantum dots dispersed in chloroform and placed in a cuvette are shown in Figure 2(a). The curves correspond to three PbSe quantum dot samples synthesized at reaction times between 20 and 40 s. The plotted absorbance spectra showed that the bandgap of the nanocrystals decreased with increasing reaction time due to the size-dependent bandgap of the colloidal nanocrystals. Four excitonic peaks were observed, arising from interband transitions between the energy bands of the quantum dots. The strong quantum confinement observed in PbSe nanocrystals is attributed to their large exciton Bohr radius of approximately 45 nm [21]. The absorbance spectrum in Figure 2(b) is for the nanocrystals used to fabricate photosensors in this work. The excitonic peaks are illustrated as k1, k2, k3, and k4. The most prominent peak (k_1) corresponds to the first interband transition following optical excitation. The small Half-Width at Half-Maximum (HWHM) of k1, calculated to be approximately 50 nm, indicates that the synthesized nanocrystals exhibit a narrow size distribution. The bandgap of these quantum dots was determined to be 0.78 eV, making them well-suited for absorption in the near-infrared region.

The absorbance spectra of the PbSe nanocrystals before and after the ligand exchange process are presented in Figure 3. The first excitonic peak (k_1) of the MAA-capped nanocrystals was red-shifted, indicating an increase in the nanocrystals' sizes during the ligand exchange process.

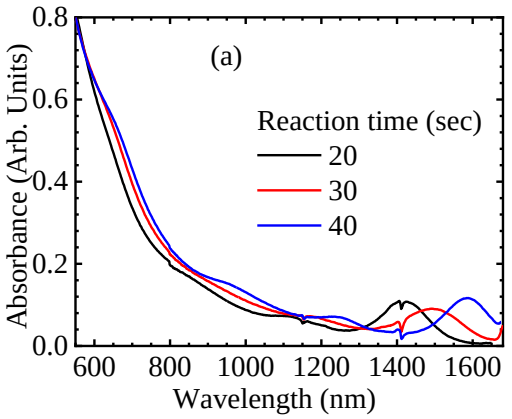

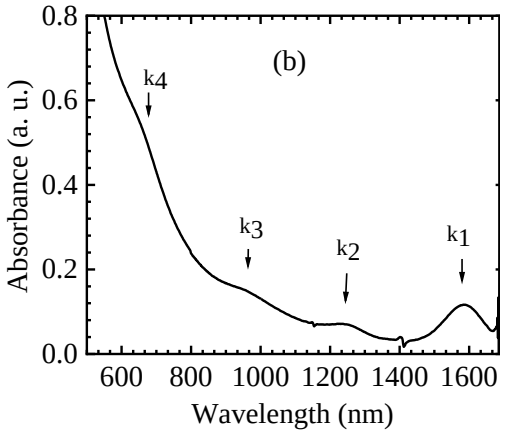

Figure 2. (a) Absorbance spectra of PbSe quantum dots synthesized at different reaction times. (b) The absorbance spectrum of PbSe quantum dots synthesized at 40 sec and used in the fabricated device.

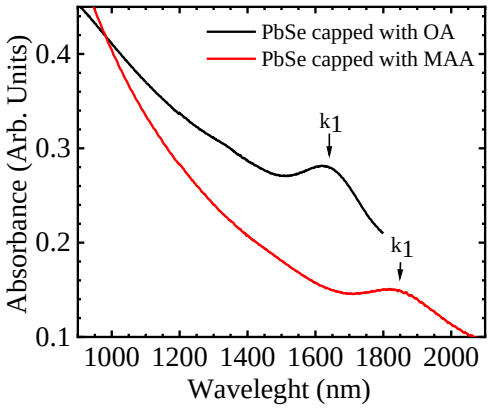

Figure 3. Absorbance spectra of PbSe quantum dots before and after ligand exchange.

Colloidal PbSe quantum dots dispersed in chloroform were drop-cast onto fabricated

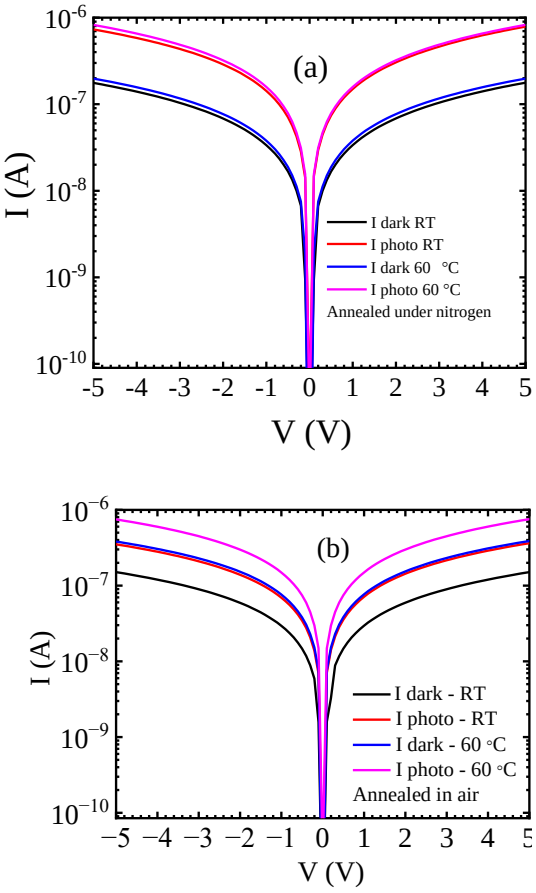

Figure 4. I–V characteristics of the fabricated PbSe quantum dot photosensor measured in the dark and under light illumination at room temperature, before and after annealing.: (a) annealed in nitrogen, (b) annealed in air.

interdigital devices with an electrode spacing of 50 µm. The I–V characteristics were then recorded over a bias range of −5 to 5 V at room temperature (RT). First, two different annealing conditions in nitrogen and in air were examined at 60 °C for 20 min, and the I-V curves were drawn in Figure 4(a) and 4(b), respectively. There was no notable change in both the photo and dark current of the device after nitrogen annealing, as shown in Figure 4(a). In contrast, air annealing increased both the dark and photocurrent compared with the RT measurements, as illustrated in Figure 4(b). The enhanced conductivity of the PbSe nanocrystal film after low-temperature air annealing is primarily due to two factors. First, the removal of residual ligands and solvents reduces interparticle spacing and improves nanocrystal ordering, facilitating better charge transport. Furthermore, this mild annealing treatment 60°C for 20 minutes, is insufficient to alter the rock-salt cubic crystal structure, known to be formed during hot-

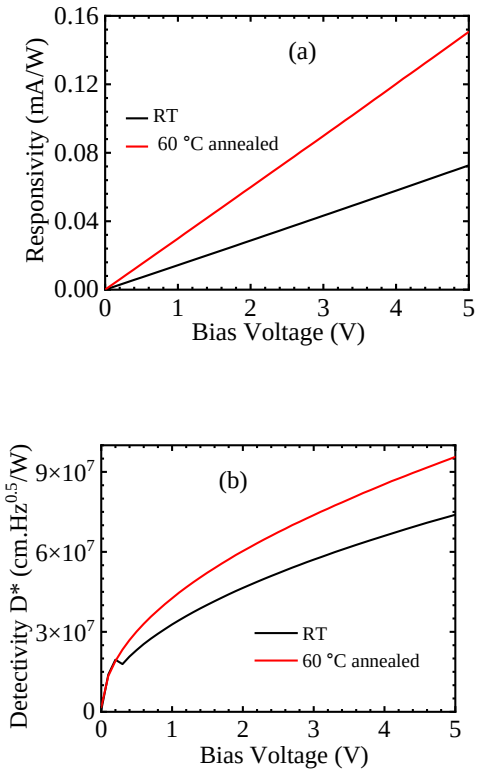

Figure 5. (a) Responsivity and (b) detectivity of the PbSe quantum dots photosensor plotted as a function of the applied bias voltage.

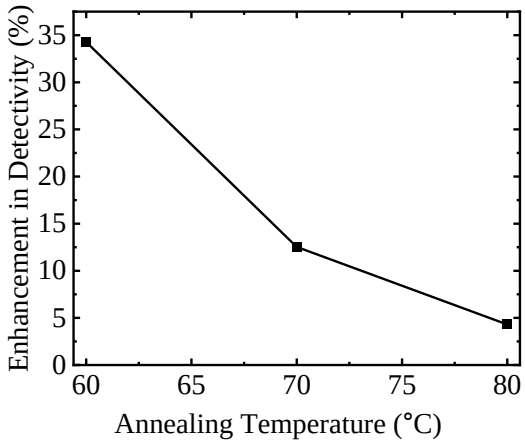

Figure 6. Percentage enhancement in conductivity of PbSe nanocrystal photodetectors

injection synthesis, or induce phase changes in solution-processed PbSe nanocrystals [15, 18]. Second, mild oxidation passivates surface trap states by forming oxide species, which suppress carrier recombination [15].

The responsivity (R) and the specific detectivity (D^*) of the photosensor annealed in air were determined using the following equations:

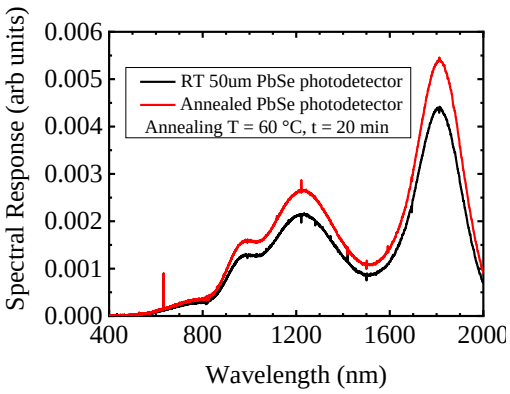

Figure 7. Spectral response of the device measured under a 5 V bias.

consistent with the absorbance characteristics presented in Figure 3. Following annealing, the enhanced optical response of the device aligns with the increased conductivity and responsivity observed in the I–V characteristics, indicating overall performance improvement.

The overall performance of our optimized photosensor was evaluated by comparing key parameters, including responsivity, specific detectivity, and processing temperature, with those reported for planar colloidal lead chalcogenide (PbSe and PbS) quantum dot photodetectors, as summarized in Table 1.

Table 1. Comparison of device performance parameters for lead-chalcogenide CQD photodetectors.

Active Material	Ligand / post-treatment	Responsivity (R)	Specific Detectivity (D∗)	Reference
PbSe QDs	MAA / Air Annealed (60 °C)	0.15 mA/W	9.5×10^7 Jones	This Work
PbSe QDs	Oleic Acid / As-cast	~ 1.2 μA/W	1.0×10^6 Jones	[19]
PbS QDs	EDT / Thermal Treatment	0.10 mA/W	1.2×10^8 Jones	[6]

$$R = \frac{I_{ph}}{P_{in}} \quad (1)$$

Where I_{ph} is the illumination current, P_{in} is the input optical power.

$$D^* = \frac{A^{\frac{1}{2}} R}{(2e\, i_d)^{\frac{1}{2}}} \quad (2)$$

A is the photosensor effective area, e is the electron charge, and i_d is the measured dark current.

Figure 5(a) and 5(b) illustrate the variation of responsivity and specific detectivity, determined based on the IV results in Figure 4(b), of the PbSe photosensor annealed in air as a function of the applied bias voltage. The responsivity and detectivity of the device had notable improvement after low-temperature annealing.

Figure 6 shows the percentage enhancement in conductivity as a function of annealing temperature for three photosensor devices annealed in air at 60 °C, 70 °C, and 80 °C for 20 min. A reduction in detectivity at higher annealing temperatures may indicate nanocrystal aggregation or over-oxidation [15, 19], though further morphological imaging such as TEM or SEM would be required to confirm this mechanism directly.

The spectral response was measured under a 5 V bias for the device annealed in air at 60 °C, both before and after the annealing process Figure 7. The result demonstrates that the PbSe quantum dot-based photosensor effectively detects the near-infrared light,

4. Conclusion

The electrical and optical properties of near-infrared photosensors based on colloidal PbSe quantum dots were systematically investigated. The quantum dots were synthesized via a hot-injection method, and long-chain oleic acid ligands were successfully exchanged with mercaptoacetic acid (MAA) to enhance interparticle charge transport. Current-voltage characteristics and spectral response measurements confirmed that the fabricated devices effectively cover the near-infrared spectrum. Low-temperature air annealing at $60°C$ significantly increased device performance, enhancing specific detectivity by approximately 35% compared to room-temperature values. However, higher annealing temperatures led to performance degradation, highlighting the need for careful thermal budget optimization to reduce interparticle spacing without causing over-oxidation or film damage. These results demonstrate that low-temperature air annealing provides a low-cost, effective strategy for optimizing colloidal quantum dot photosensors.

5. Acknowledgement

The author would like to acknowledge the Optoelectronics Research Lab at the University of Arkansas, USA, for providing the laboratory facilities and research environment necessary to conduct the experiments presented in this work.

References

[1] J. Mathews, R. Roucka, J. Xie, S. Q. Yu, J. Méndez, and J. Kouvetakis, "Extended performance GeSn/Si(100) p-i-n photodetectors for full spectral range telecommunication applications," Appl. Phys. Lett., vol. 95, no. 13, art. no. 133501, pp. 1–4, Oct. 2009. https://doi.org/10.1063/1.3238327

[2] D. M. Shcherbakova and V. V. Verkhusha, "Near-infrared fluorescent proteins for multicolor in vivo imaging," Nat. Methods, vol. 10, no. 8, pp. 751–754, Aug. 2013. https://doi.org/10.1038/nmeth.2521

[3] H. Gong et al., "Near-infrared fluorescence imaging of mammalian cells and xenograft tumors with SNAP-tag," PLoS One, vol. 7, no. 3, art. no. e34003, Mar. 2012. https://doi.org/10.1371/journal.pone.0034003

[4] G. B. Shan and G. P. Demopoulos, "Near-infrared sunlight harvesting in dye-sensitized solar cells via the insertion of an upconverter-TiO2 nanocomposite layer," Adv. Mater., vol. 22, no. 39, pp. 4373–4377, Aug. 2010. https://doi.org/10.1002/adma.201001816

[5] F. H. L. Koppens, T. Mueller, P. Avouris, A. C. Ferrari, M. S. Vitiello, and M. Polini, "Photodetectors based on graphene, other two-dimensional materials and hybrid systems," Nat. Nanotechnol., vol. 9, no. 10, pp. 780–793, Oct. 2014. https://doi.org/10.1038/nnano.2014.215

[6] A. De Iacovo, C. Venettacci, L. Colace, L. Scopa, and S. Foglia, "PbS colloidal quantum dot photodetectors operating in the near infrared," Sci. Rep., vol. 6, art. no. 37913, Nov. 2016. https://doi.org/10.1038/srep37913

[7] M. Chen et al., "Mercury telluride quantum dot-based phototransistor enabling high-sensitivity room-temperature photodetection at 2000 nm," ACS Nano, vol. 11, no. 6, pp. 5614–5622, May 2017. https://doi.org/10.1021/acsnano.7b00972

[8] P. H. Chang et al., "Ultrahigh responsivity and detectivity graphene–perovskite hybrid phototransistors by sequential vapor deposition," Sci. Rep., vol. 7, art. no. 46281, Apr. 2017. https://doi.org/10.1038/srep46281

[9] G. Konstantatos and E. H. Sargent, "Nanostructured materials for photon detection," Nat. Nanotechnol., vol. 5, no. 6, pp. 391–400, Jun. 2010. https://doi.org/10.1038/nnano.2010.78

[10] W. Gebril and M. O. Manasreh, "Self-powered graphene phototransistor with high and tunable responsivity and detectivity," Eng. Res. Express, vol. 3, no. 1, art. no. 015022, Feb. 2021. https://doi.org/10.1088/2631-8695/abe218

[11] J. P. Clifford, G. Konstantatos, K. W. Johnston, S. Hoogland, L. Levina, and E. H. Sargent, "Fast, sensitive and spectrally tuneable colloidal-quantum-dot photodetectors," Nat. Nanotechnol., vol. 4, no. 1, pp. 40–44, Jan. 2009. https://doi.org/10.1038/nnano.2008.313

[12] R. B. Vasiliev, S. G. Dorofeev, D. N. Dirin, D. A. Belov, and T. A. Kuznetsova, "Synthesis and optical properties of PbSe and CdSe colloidal quantum dots capped with oleic acid," Mendeleev Commun., vol. 14, no. 4, pp. 169–171, Jul.–Aug. 2004. https://doi.org/10.1070/MC2004V014N04ABEH001970

[13] W. Gebril, H. Salman, and M. O. Manasreh, "Near-infrared photodetectors based on hybrid graphene-colloidal PbSe quantum dots," MRS Adv., vol. 5, no. 44, pp. 2273–2280, Nov. 2020. https://doi.org/10.1557/adv.2020.256

[14] S. Yakunin et al., "High infrared photoconductivity in films of arsenic-sulfide-encapsulated lead-sulfide nanocrystals," ACS Nano, vol. 8, no. 12, pp. 12883–12894, Dec. 2014. https://doi.org/10.1021/nn5067478

[15] M. Law, J. M. Luther, Q. Song, B. K. Hughes, C. L. Perkins, and A. J. Nozik, "Structural, optical, and electrical properties of PbSe nanocrystal solids treated thermally or with simple amines," J. Am. Chem. Soc., vol. 130, no. 18, pp. 5974–5985, May 2008. https://doi.org/10.1021/ja800040c

[16] F. Hetsch, N. Zhao, S. V. Kershaw, and A. L. Rogach, "Quantum dot field effect transistors," Mater. Today, vol. 16, no. 9, pp. 312–325, Sep. 2013. https://doi.org/10.1016/j.mattod.2013.08.011

[17] R. R. Knauf, J. C. Lennox, and J. L. Dempsey, "Quantifying ligand exchange reactions at CdSe nanocrystal surfaces," Chem. Mater., vol. 28, no. 13, pp. 4762–4770, Jul. 2016. https://doi.org/10.1021/acs.chemmater.6b01827

[18] J. M. Luther, M. Law, Q. Song, C. L. Perkins, M. C. Beard, and A. J. Nozik, "Structural, optical, and electrical properties of self-assembled films of PbSe nanocrystals treated with 1,2-ethanedithiol," ACS Nano, vol. 2, no. 2, pp. 271–280, Feb. 2008. https://doi.org/10.1021/nn7003348

[19] M. S. Kang, A. Sahu, D. J. Norris, and C. D. Frisbie, "Size- and temperature-dependent charge transport in PbSe nanocrystal thin films," Nano Lett., vol. 11, no. 9, pp. 3887–3892, Sep. 2011. https://doi.org/10.1021/nl2020153

[20] W. W. Yu, J. C. Falkner, B. S. Shih, and V. L. Colvin, "Preparation and characterization of monodisperse PbSe semiconductor nanocrystals in a noncoordinating solvent," Chem. Mater., vol. 16, no. 17, pp. 3318–3322, Aug. 2004. https://doi.org/10.1021/cm049476y

[21] F. W. Wise, "Lead salt quantum dots: the limit of strong quantum confinement," Acc. Chem. Res., vol. 33, no. 11, pp. 773–780, Nov. 2000. https://doi.org/10.1021/ar970220q